Supplementary information

Preparation of Few-Layer Bismuth Selenide by Liquid-Phase-Exfoliation and Its Optical Absorption Properties

Liping Sun[1], Zhiqin Lin[1], Jian Peng[1], Jian Weng[1,3]*, Yizhong Huang[2], Zhengqian Luo[2]*

[1]Department of Biomaterials, College of Materials, Xiamen University, Xiamen 361005, China.

[2]Institute of Optoelectronic Technology, Department of Electronic Engineering, Xiamen University, Xiamen 361005, China.

[3]ShenZhen Research Institute of Xiamen University, Shenzhen 518057, China

Correspondence and requests for materials should be addressed to J.W. (e−mail: jweng@xmu.edu.cn) or Z.Q.L. (e-mail: zqluo@xmu.edu.cn).

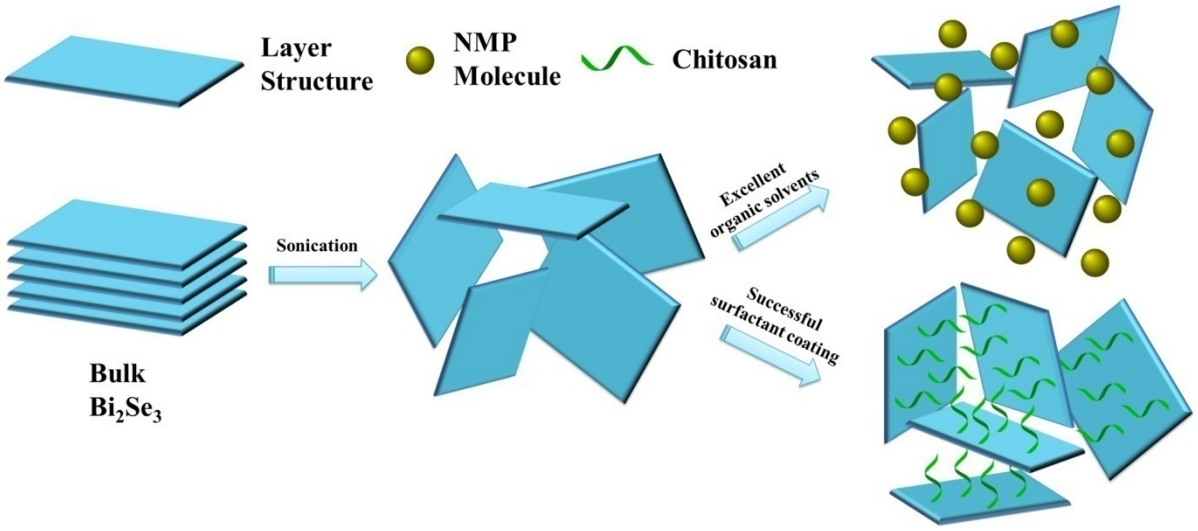

Supplementary Figure S1 | Schematic of liquid-phase exfoliation. Bulk Bi_2Se_3 is sonicated in solvents to produce few-layer Bi_2Se_3. In organic solvent, NMP with an appropriate surface tension plays an important role to exfoliate bulk Bi_2Se_3 into stabilized nanosheets against reaggregation. In acetic solution of chitosan, chitosan as a surfactant can be adsorbed on the surface of few-layer Bi_2Se_3 to avoid its reaggregation.

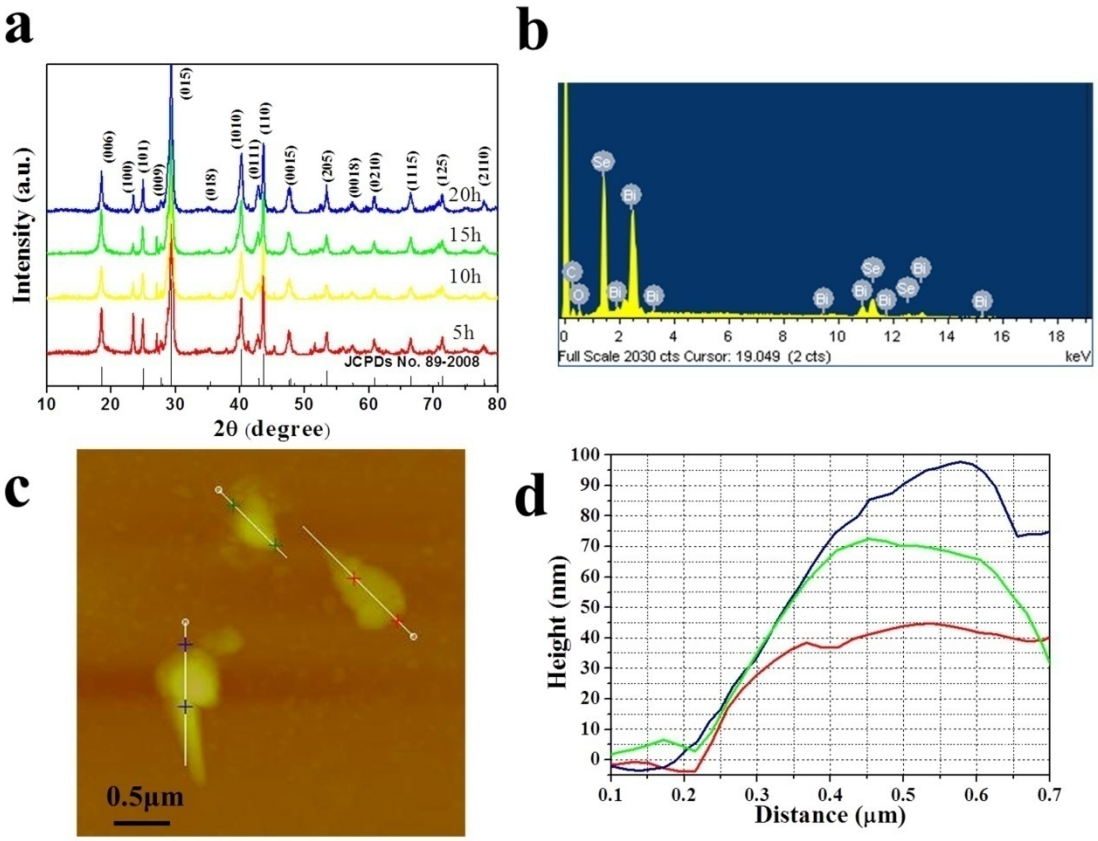

Supplementary Figure S2 | Characterization of as-synthesized bulk Bi_2Se_3. (a) XRD patterns of bulk Bi_2Se_3 prepared at different reaction times. The XRD patterns were readily indexed to rhombohedral Bi_2Se_3 (JCPDS no. 89-2008). The strong and sharp peaks of samples indicate that the as-synthesized bulk Bi_2Se_3 was crystalline. (b) Energy dispersive X-ray spectrum of as-synthesized bulk Bi_2Se_3. The atomic ratio of Bi and Se is 1:1.58 that is close to the theoretically atomic ratio (1.5) in Bi_2Se_3, which is consistent with the result of XRD. (c, d) AFM image and the corresponding height profiles of as-synthesized bulk Bi_2Se_3 with several tens of nanometers in thickness.

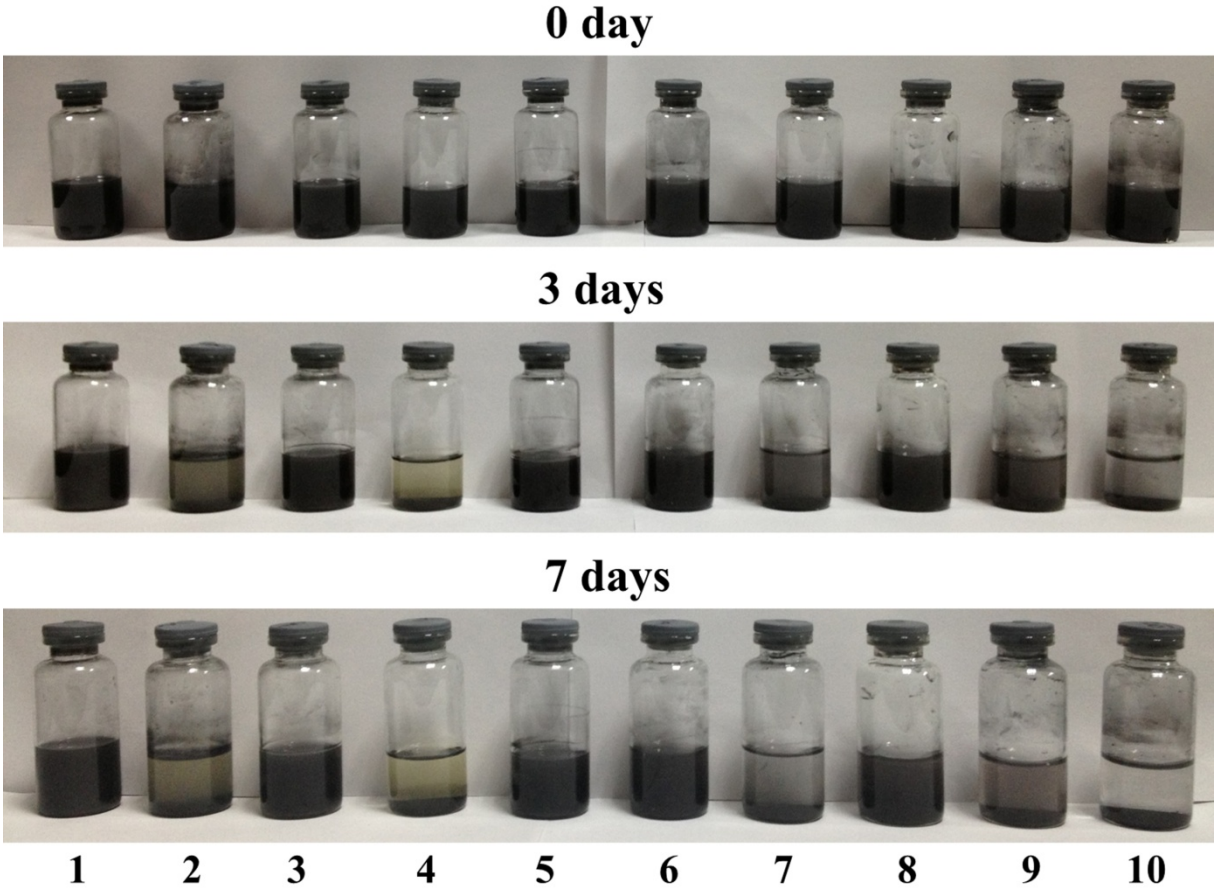

Supplementary Figure S3 | Exfoliating as-synthesized bulk Bi_2Se_3 with different solvents. Ten solvents were used to exfoliate Bi_2Se_3 with same ultrasonic time and concentration. These solvents were NMP, styrene, methanol, acetone, isopropanol, CS-HAc, Pluronic® P-123, poly(sodium 4-styrenesulfonate), sodium cholate and deionized water, respectively (numbering them 1-10 from left to right). Bi_2Se_3 powder was added into 20 ml of cylindrical vial (1 $mg \cdot mL^{-1}$), then sonicating for 30 h. Photographs show the disperse state of Bi_2Se_3 in different solvents standing for different days after sonication. Bi_2Se_3 can be exfoliated in NMP, methanol, isopropanol, CS-HAc and poly(sodium 4-styrenesulfonate). The colors of NMP and CS-HAc are deepest in all solvents. Therefore, NMP and CS-HAc are used in following experiments.

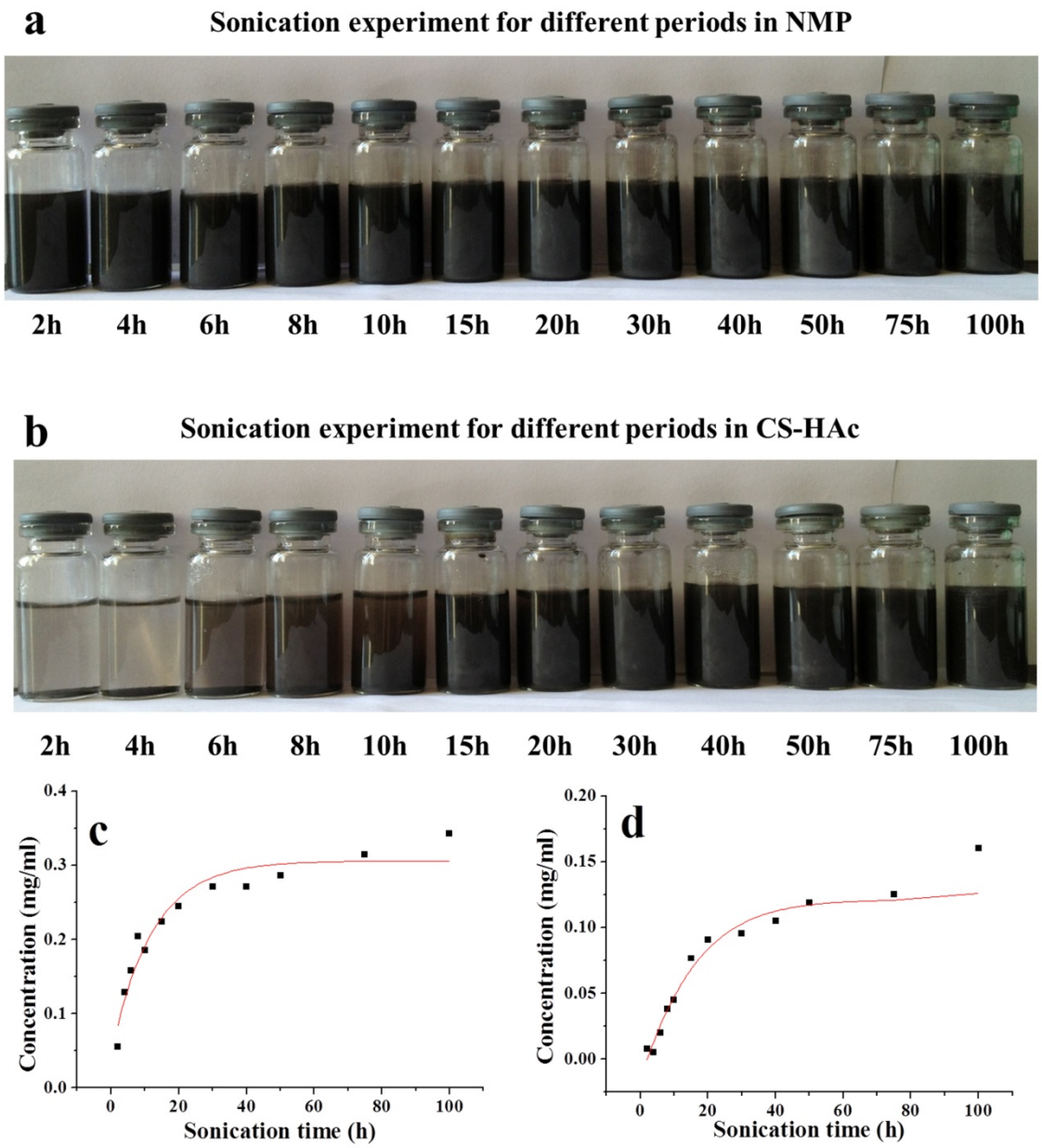

Supplementary Figure S4 | Effect of ultrasonic time on exfoliation of as-synthesized bulk Bi_2Se_3. (a) The photograph of Bi_2Se_3 with different sonication times in NMP. (b) The photograph of Bi_2Se_3 with different sonication times in CS-HAc. (c) The produced few-layer Bi_2Se_3 with different sonication times in NMP. (d) The produced few-layer Bi_2Se_3 with different sonication times in CS-HAc. The calculated absorption coefficient α at 574 nm is 1378 mL mg^{-1} m^{-1}.

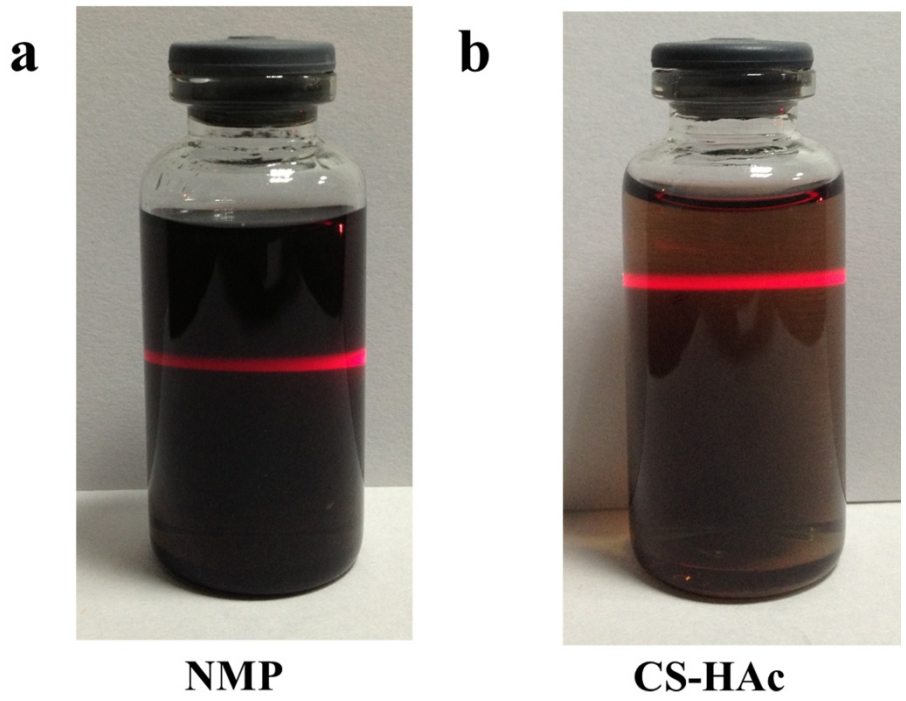

Supplementary Figure S5 | Typical Tyndall effect of few-layer Bi_2Se_3 colloidal suspension.

(a) Few-layer Bi_2Se_3 dispersed in NMP. (b) Few-layer Bi_2Se_3 dispersed in CS-HAc.

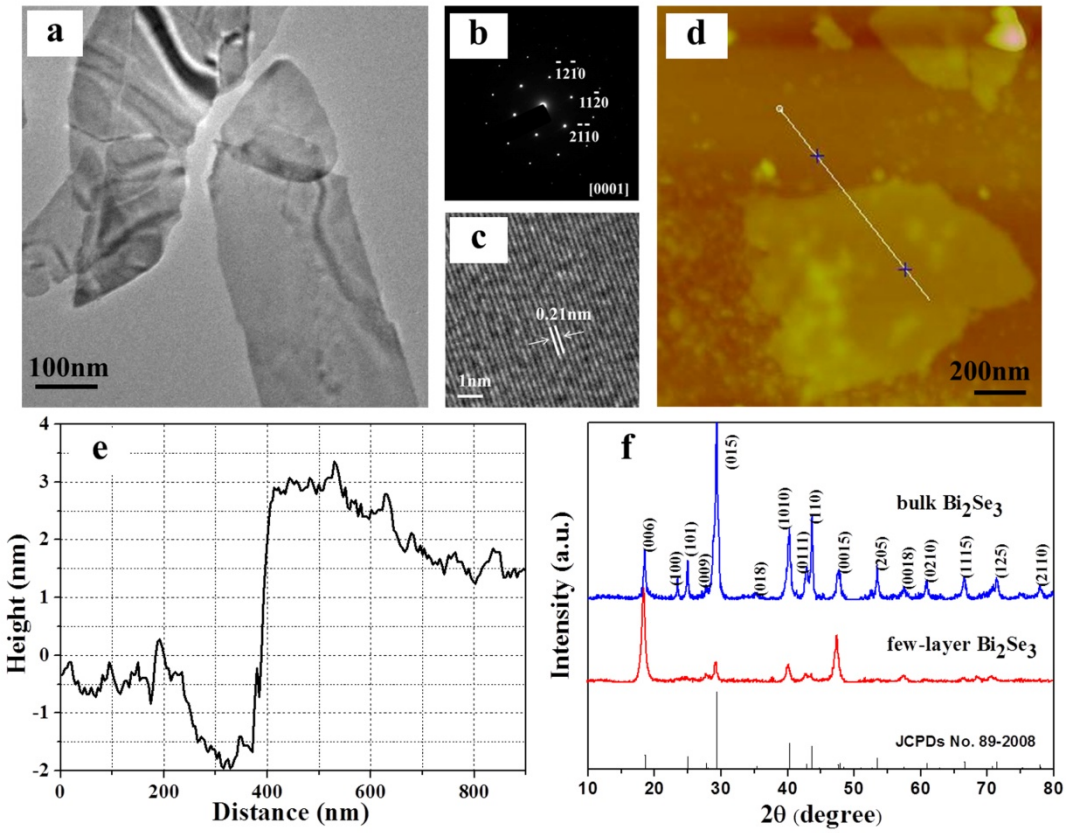

Supplementary Figure S6 | Confirmation of few-layer Bi_2Se_3 exfoliated in CS-HAc. (a) TEM image of few-layer Bi_2Se_3. (b) SAED pattern of few-layer Bi_2Se_3. (c) HRTEM image of few-layer Bi_2Se_3. (d, e) AFM image and the corresponding height profile of few-layer Bi_2Se_3 with a thickness of ca. 3~4 nm. (f) XRD pattern of few-layer Bi_2Se_3.

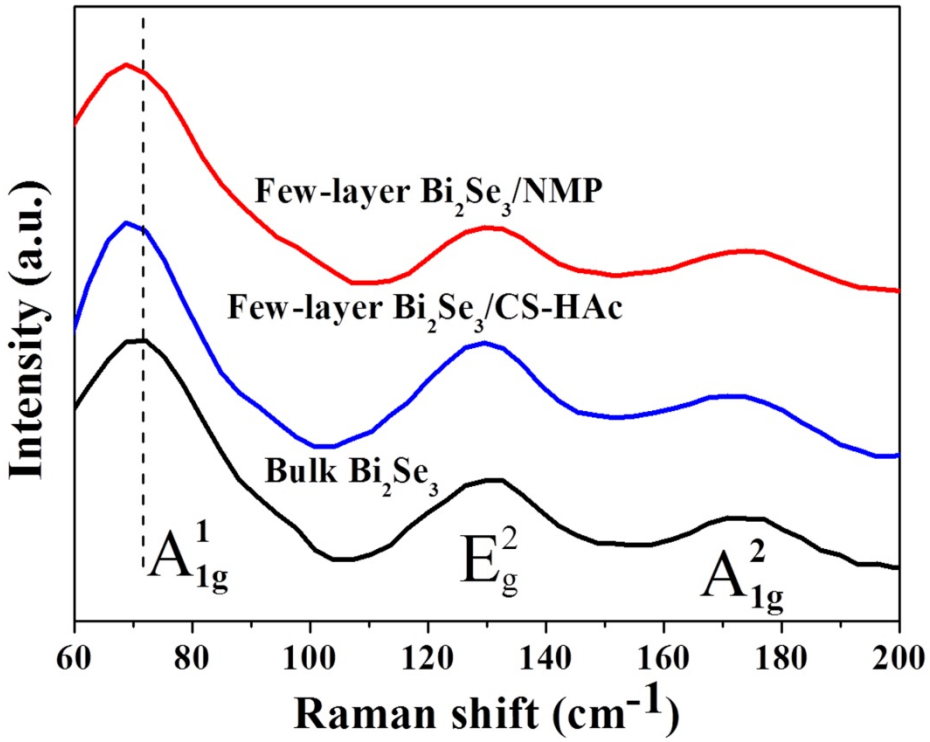

Supplementary Figure S7 | Raman spectra of as-synthesized bulk and few-layer Bi_2Se_3. The peak of bulk Bi_2Se_3 at ~72, ~131, and~174 cm^{-1}, are assigned to A^1_{1g}, E^2_g and A^2_{1g} vibrational modes, respectively. The dashed vertical line indicates red shift of A^1_{1g} mode in few-layer Bi_2Se_3 from bulk Bi_2Se_3.

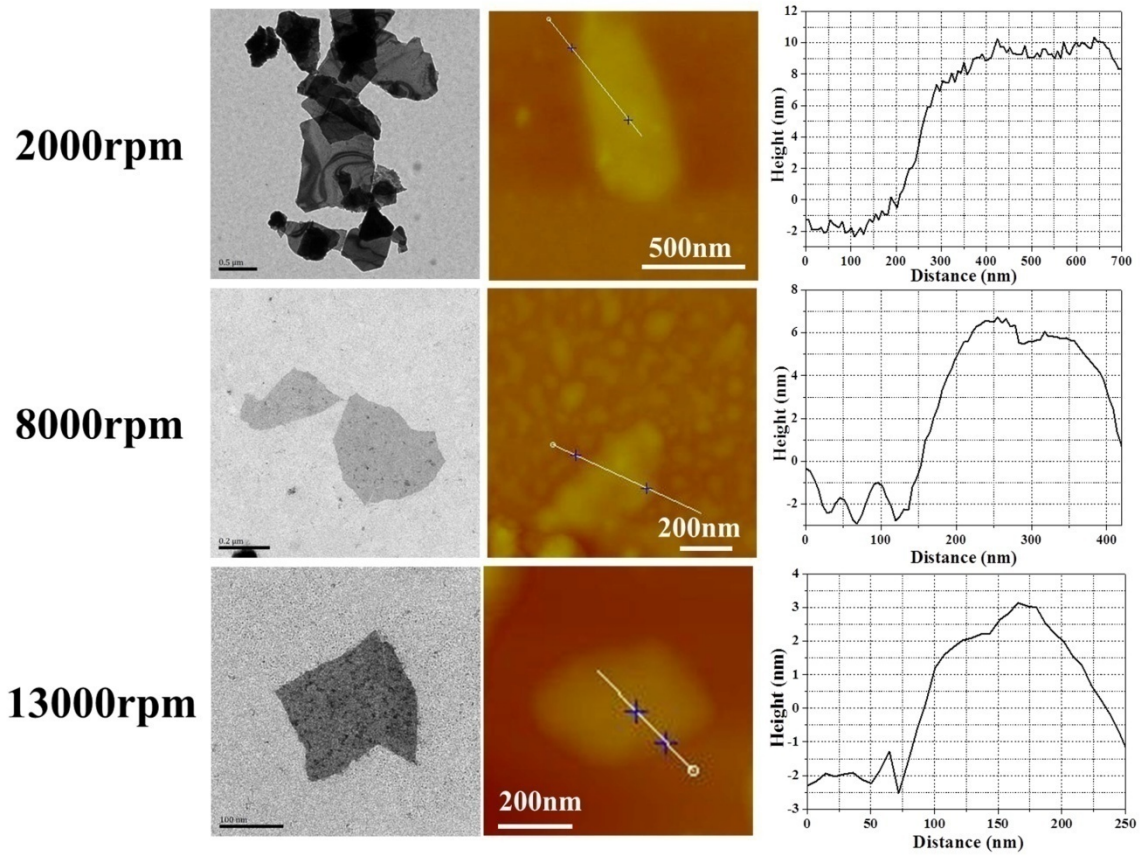

Supplementary Figure S8 | TEM and AFM images and the corresponding height profiles of few-layer Bi_2Se_3 in CS-HAc collected with different centrifugal speeds. Three few-layer Bi_2Se_3 solutions were obtained with the same treatment in Fig. 4. The result is similar to that in NMP.

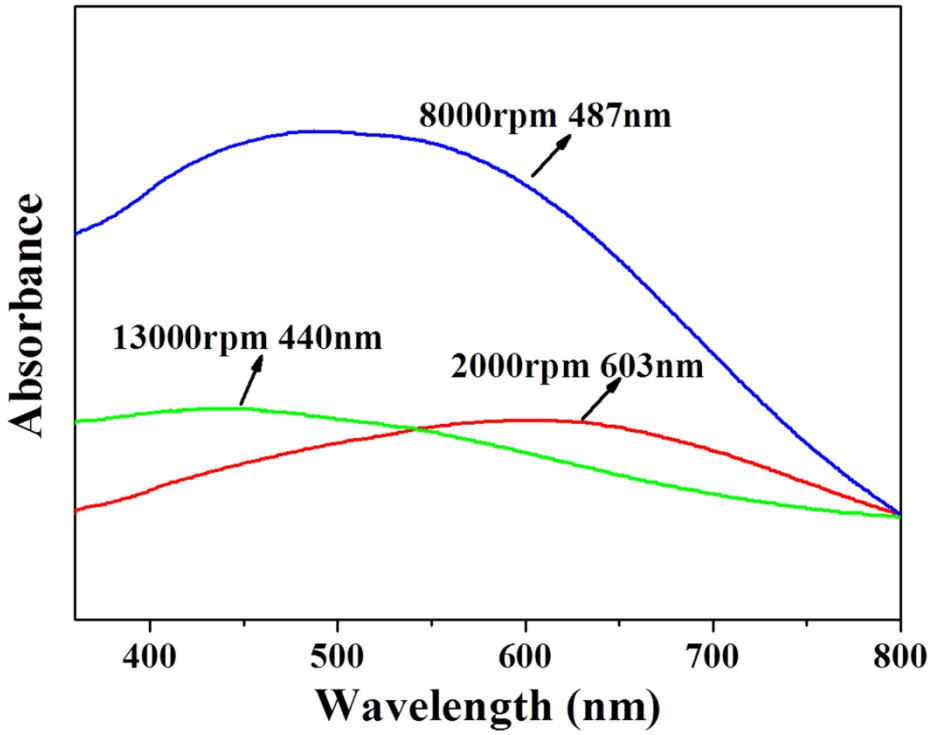

Supplementary Figure S9 | UV-vis absorption spectra of few-layer Bi_2Se_3 in CS-HAc collected with different centrifugal speeds. In the visible absorption spectra, the absorption band of three samples were 603 (red curve), 487 (blue curve) and 440 nm (green curve) corresponding to 2000, 8000 and 13000 rpm, respectively. The result is similar to that in NMP (Fig. 4).

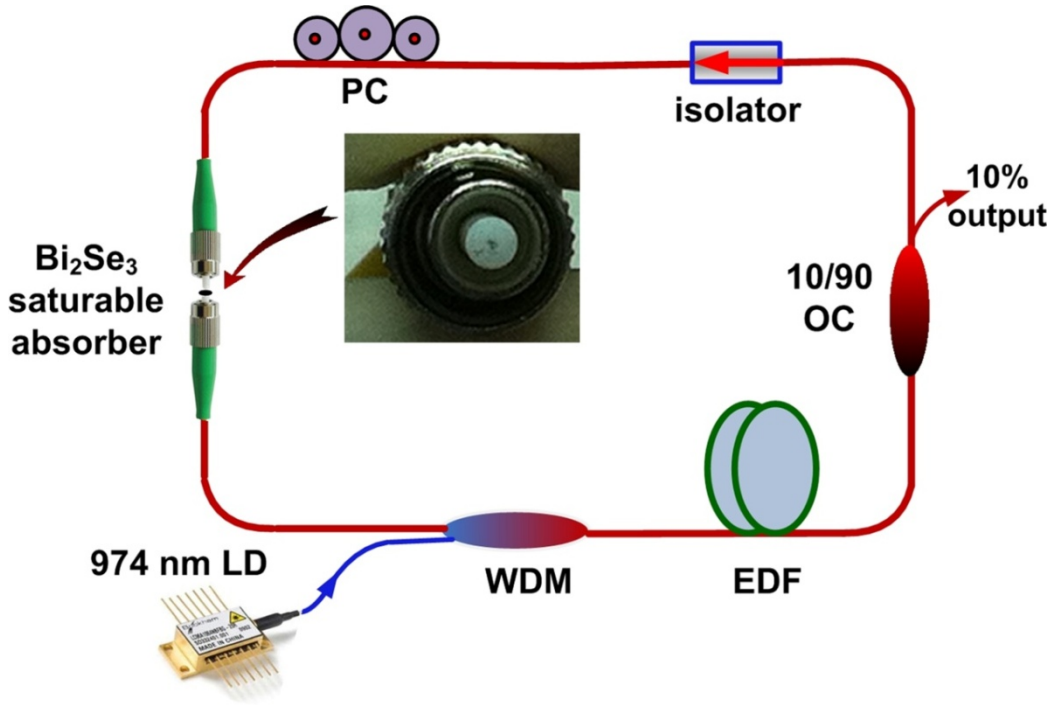

Supplementary Figure S10 | Experimental setup of few-layer Bi_2Se_3-based Q-switched EDFL. The fiber ring laser is schematically described here (Inset: the image of few-layer Bi_2Se_3-deposited fiber ferrule). A section of 4.1 m erbium-doped fiber (EDF, Nufern EDFC-980-HP) was pumped by a 200 mW/974 nm laser diode (LD, Bookham Inc.) through a 976/1530 nm wavelength division multiplexer (WDM), for providing the laser gain in 1.5 μm waveband. A 10/90 optical coupler (OC, EPTEK Co. Ltd.) operating in the range of 1520-1570 nm was used to output 10% Q-switched laser. An optical isolator (Thorlabs, IO-H-1550) can block any undesired reflection and also ensure the unidirectional operation. A polarization controller (PC, Thorlabs FPC030) was used to optimize the laser operation. Few-layer Bi_2Se_3 was inserted into the laser cavity as a passive Q-switcher. The Bi_2Se_3 saturable absorber device was fabricated by optically depositing the few-layer Bi_2Se_3 or as-synthesized bulk Bi_2Se_3 onto a fiber ferrule. As shown in the inset, Bi_2Se_3 can be well deposited on the central core of fiber. The insertion losses of few-layer Bi_2Se_3 and as-synthesized bulk Bi_2Se_3 devices are 2.5 and 2.4 dB, respectively.

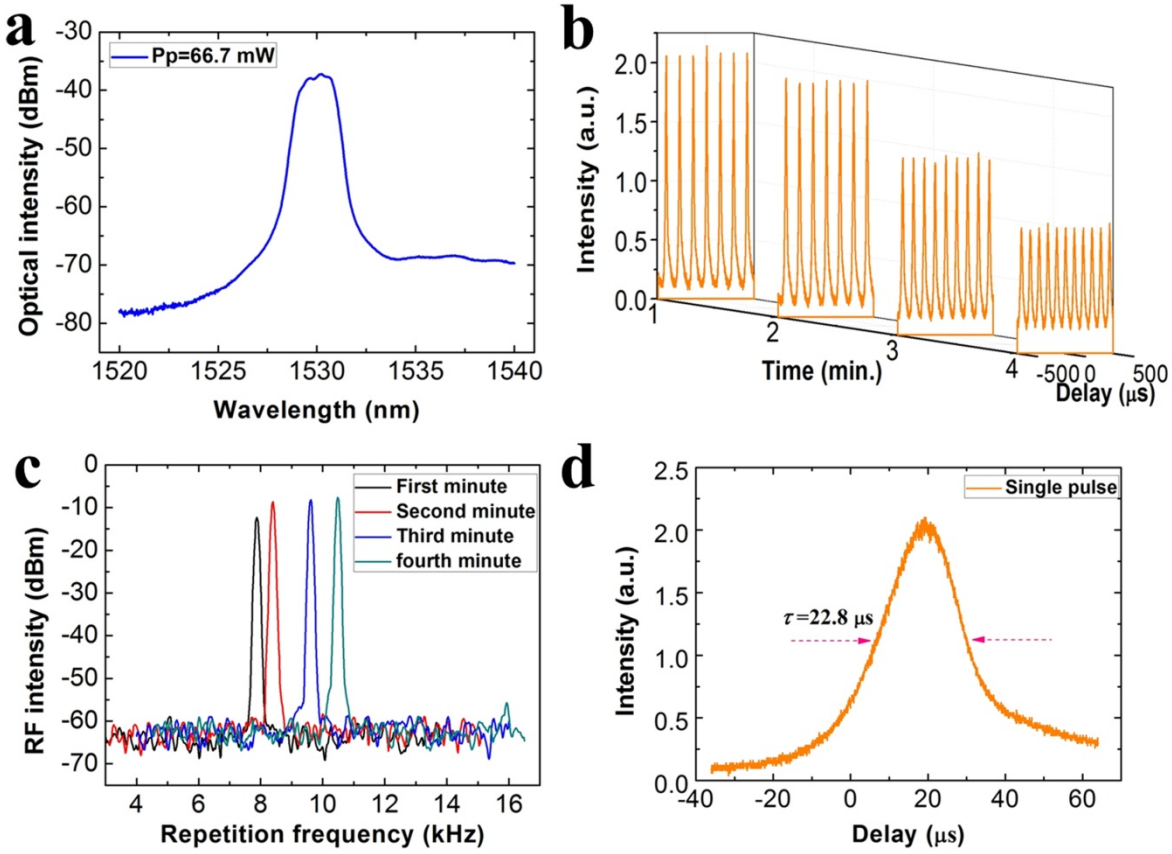

Supplementary Figure S11 | Unstable Q-switching operation with as-synthesized bulk Bi_2Se_3. Unstable Q-switching operation was observed using bulk Bi_2Se_3 at the pump power of 66.7 mW. (a) The optical spectrum of Q-switching; (b) Unstable Q-switched pulsed trains recorded at a 1 min interval; (c) Unstable repetition rate recorded at a 1 min interval; (d) The obtained minimum pulse duration of Q-switching.

When as-synthesized bulk Bi_2Se_3 was deposited on a fiber ferrule and then inserted into the laser cavity in Fig. S10, an unstable Q-switching operation was observed. Such laser started the CW lasing at the pump threshold of 9.2 mW, but it transmitted to the Q-switching operation at the higher pump power of 22.1 mW. At the pump power of 66.7 mW, we

recorded the typical characteristics of such Q-switching with bulk Bi_2Se_3, as shown in Fig. S11. The laser spectrum of this Q-switching (Supplementary Fig. S11a) has the central wavelength of 1530.2 nm which is same to that of few-layer Bi_2Se_3 (Fig. 6c), due to the similar insertion loss (~2.5 dB). As given in Supplementary Fig. S11b, the oscilloscope traces of Q-switching at the same pump power of 66.7 mW were recorded at a 1 min interval. One can clearly see that the pulse intensity gradually declined. Moreover, the pulsed repetition rate became higher from 7.8 to 10.3 kHz as correspondingly measured by the RF spectrum analyzer. These results indicate that this Q-switching operation using bulk Bi_2Se_3 is very unstable, having the strong fluctuations of both the pulse intensity and repetition rate. The minmum pulse duration of such Q-switching is 22.8 μs (Supplementary Fig. S11d) and is much broader than that of few-layer Bi_2Se_3 (4.9 μs, Fig. 6f). More importantly, the Q-switching operation is limited to a small range of pump power (22.1~67.5 mW).

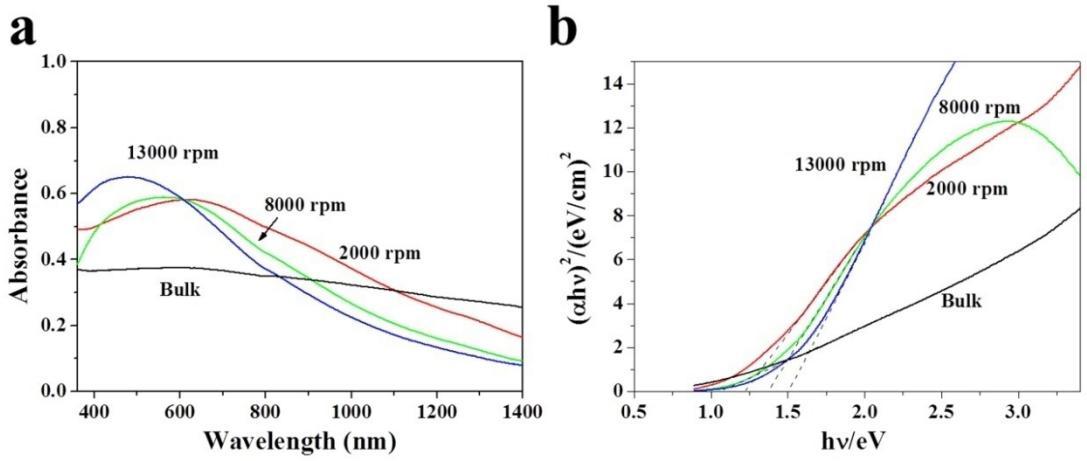

Supplementary Figure S12 | The E_g for different few-layer Bi_2Se_3 in NMP collected with different centrifugal speeds. (a) Plots of absorption *vs.* wavelength of Bi_2Se_3 in the UV-Vis-NIR region. (b) Plot of $(\alpha h\nu)^2$ *vs.* hν for different size of Bi_2Se_3. The values of E_g were determined by extrapolating the straight portion of the plot to the energy axis in (b).

Supplementary Table S1 | E_g of Bi_2Se_3 with different thickness in NMP.

	Bulk (calculated)	Bulk (as-synthesized)	2000 rpm	8000 rpm	13000 rpm
Thickness (nm)	>10 μm	40-100	9.6	5.76	1.92
E_g (eV)	0.3	1.08	1.22	1.39	1.50
R (nm)	/	/	182.48	146.6	21.79

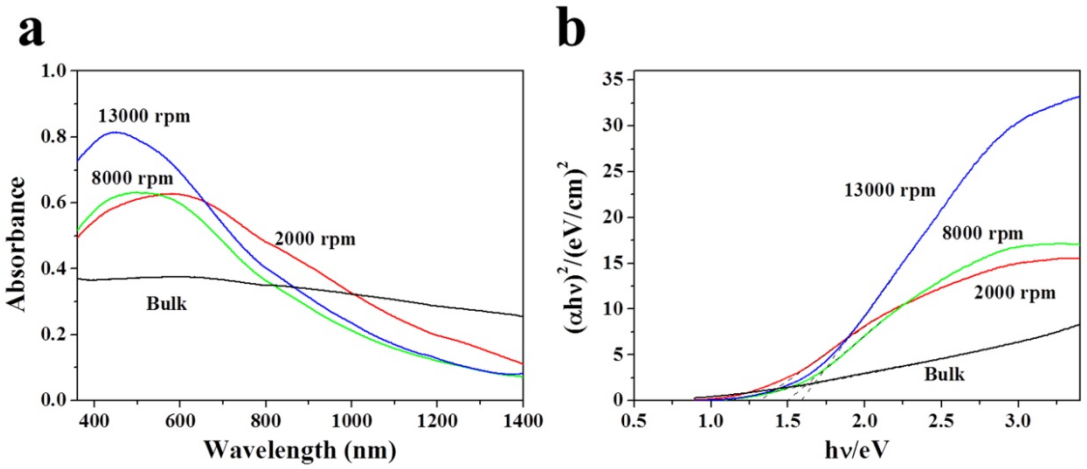

Supplementary Figure S13 | The band gap E_g for different few-layer Bi_2Se_3 in CS-HAc collected with different centrifugal speeds. (a) Plots of absorption *vs.* wavelength of Bi_2Se_3 in the UV-Vis-NIR region. (b) Plot of $(\alpha h\nu)^2$ *vs.* hν for different size of Bi_2Se_3. The values of E_g were determined by extrapolating the straight portion of the plot to the energy axis in (b).

Supplementary Table S2 | E_g of Bi_2Se_3 in CS-HAc.

	Bulk (calculated)	Bulk (as-synthesized)	2000 rpm	8000 rpm	13000 rpm
Thickness (nm)	>10 μm	40-100	9.6	5.76	1.92
E_g (eV)	0.3	1.08	1.33	1.51	1.59
R (nm)	/	/	322.63	201.64	26.54

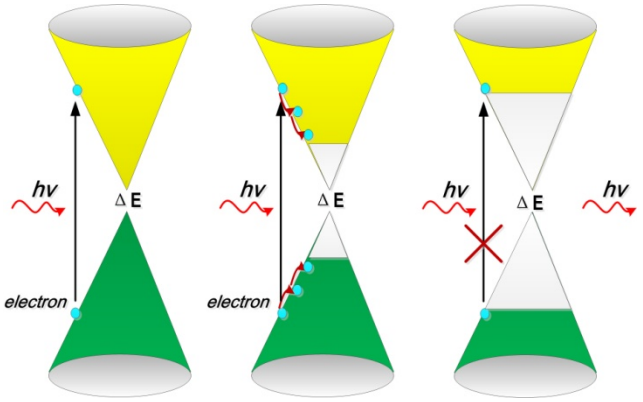

Supplementary Fig. S14 | Schematic for describing the principle of saturable absorption of few-layer Bi_2Se_3 under the light excitation. Under strong light excitation, the electrons in the valence band become depleted while the finial state in the conduction band is partially occupied, and further excitation from the valence band is blocked and no further absorption is induced, leading to a saturable absorption effect.

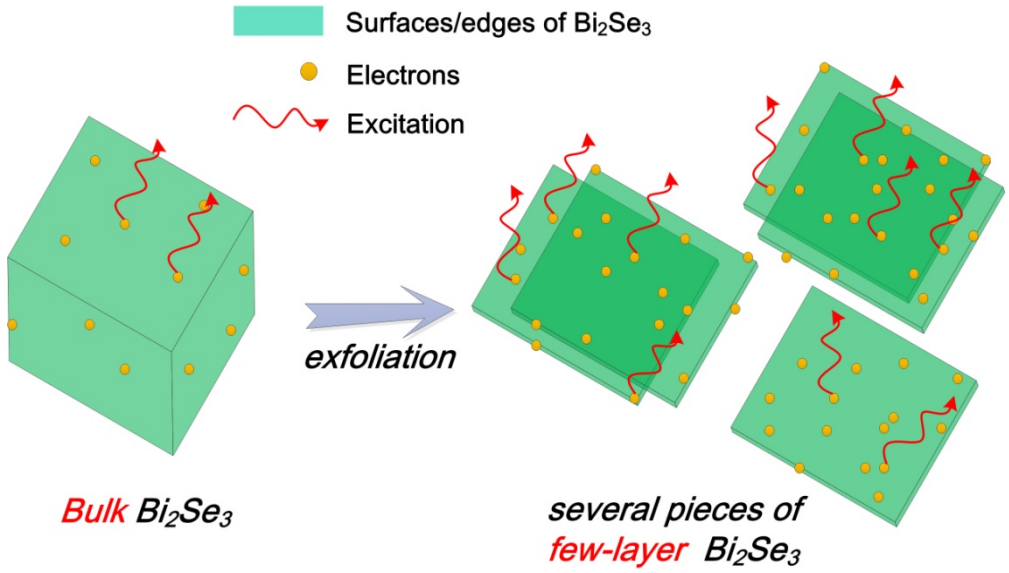

Supplementary Fig. S15 | The illustration why the optically saturable absorption of few-layer Bi_2Se_3 is superior to that of as-synthesized bulk Bi_2Se_3. Bulk Bi_2Se_3 can be exfoliated to many few-layer Bi_2Se_3 sheets, in this process the surfaces/edges can be sharply increased. Under light excitation, the surface electrons of few-layer Bi_2Se_3 can be transited more readily, because few-layer Bi_2Se_3 possesses more metallic surfaces/edges in comparison with the bulk one.